***Research Article***

Chemical Review and Letters
journal homepage: www.chemrevlett.com
ISSN (online): 2645-4947 (print) 2676-7279

# Thermodynamics and kinetics of 1-fluoro-2-methoxypropane with Bromine monoxide radical (BrO•)

Adamu Uzairu[a], Adamu Gideon Shallangwa [a], Yakub Azeh [b], Sani Uba [a], Mohammed Rufai Abubakar [a, *]

[a] *Department of Chemistry, Ahmadu Bello University, Zaria, Nigeria*
[b] *Department of Chemistry, Ibrahim Badamasi Babangida University, Lapai, Nigeria*

ARTICLE INFO

*Article history:*
Received
Received in revised form
Accepted
Available online

*Keywords:*
DFT
CFCs
1-fluoro-2-methoxypropane
Bromine monoxide radical

ABSTRACT

CFCs containing volatile compounds are detrimental to atmospheric environment and to all living organisms. Their photodissociation reactions result to reasonable amount of Chlorine atoms formation in the stratospheric part of atmosphere.
In this work, an Insilco investigation was conducted on the thermochemistry, mechanism and kinetics of the Hydrogen abstraction reactions of partially fluorinated isopropyl methyl ether (1-fluoro-2-methoxypropane i.e. ($CH_2FCH(OCH_3)CH_3$)) with Bromine monoxide radical (BrO•) using the Density Functional Theory (DFT) based M06-2X/6-311++G** strategy. To computationally refine the energy data, the single-point calculations (DFT/M06-2X/6-311++G(2df,2p) were immediately executed on the reacting species involved. The Monte Carlo search on the investigating $CH_2FCH(OCH_3)CH_3$ showed nine conformers with the global minimum configuration being studied.
The computed total theoretical rate of $7.95*10^{-11}$ $M^{-1}$ $sec^{-1}$ with atmospheric lifetime/global warming potential of $1.35*10^{-2}$ days/72.8 were also reported. The energy profile diagram of each reaction route with the BrO• was sketched at absolute temperature of 298.15 K.

## 1. Introduction

The volatile organic compounds (VOCS) released into atmosphere often undergo primary degradation through oxidation with atmospheric radicals e.g. •OH, ClO•, BrO•, $NO_3$, •$OH_2$, $RO_2$ etc. [1-5]. Recently added knowledge by [6] on ozone chemistry revealed that aerosols: deodorant sprays, paint sprays, furniture polishes, refrigerators etc. cause environmental setback on ozone ($O_3$) due to usage of chlorofluorocarbons (CFCs) during their productions. They cause this environmental havoc by diffusing into $O_3$ layer and thus deplete it at a rate faster than it (ozone) can be replaced in the atmosphere [7-14]. For this reason, international warning and restrictions were placed on the application of CFCs as agreed upon in the Montreal Protocol [15-17]. Instead, alternative chemicals with zero or less posing ability on ozone were recommended as substantial substitutes for the CFCs [18-21]. Currently, oxygenated hydrofluoroethers (HFEs) [22], have been discovered as substantial substitutes for CFCs with numerous applications ranging from refrigerators, cleaning agents, propellants, painting, solvents, pesticides, varnishes in laboratories etc. [23-28]. The presence of $-O-$ linkage between these series increases their chemical reactivity in the atmosphere which account for the chemistry of their short lifetime and lesser atmospheric effects compared to CFCs [29-33].

An investigation of $CFH_2CH(OCH_3)CH_3$ with BrO• radical is a vital atmospheric oxidation reaction that will helps in the provision of data regarding the tropospheric reactivity and degradation pathways of it in the atmosphere. Therefore, it is necessary to look into the atmospheric chemistry of it for proper understanding of this sample as a compound capable of replacing CFCs, and possibly estimate its atmospheric lifetime and global warming potentials.

Numerous wet laboratory studies investigated on the related study of this type only succeeded in providing

* Corresponding author. Tel.: +234-7033748067; e-mail: marufai2424@gmail.com

the overall rate constants but found it very difficult to reveal the actual mechanism and the true reaction picture especially when the reaction follows multiple routes. However, with simple computational approach the detailed mechanism, thermochemistry of multiple route reactions as well as overall rate constant can be estimated accurately at a time. This computational approach is very easy, cost and time saver, very fast and characterized with high accuracy when compares to wet laboratory approach.

The main objective of this investigation was to make a systematic computational kinetic study on reaction of $CFH_2CH(OCH_3)CH_3$ with $BrO^{\bullet}$ radical using easy computational techniques. And also aimed at studying the computational kinetics of H-abstraction reaction of $CFH_2CH(OCH_3)CH_3$ by $BrO^{\bullet}$ radical which involves four (4) H-abstraction positions of $-OCH_3, -CH_2F, -CH$ and $-CH_3$ as shown in the chemical reactions in equation 1-4.

$$CFH_2CH(OCH_3)CH_3 + BrO \rightarrow CFHCH(OCH_2)CH_3 + HOBr \quad (1) \quad k_1$$
$$CFH_2CH(OCH_3)CH_3 + BrO \rightarrow CFH_2C(OCH_3)CH_3 + HOBr \quad (2) \quad k_2$$
$$CFH_2CH(OCH_3)CH_3 + BrO \rightarrow CFH_2CH(OCH_3)CH_2 + HOBr \quad (3) \quad k_3$$
$$CFH_2CH(OCH_3)CH_3 + BrO \rightarrow CFH_2CH(OCH_2)CH_3 + HOBr \quad (4) \quad k_4$$

## 2. Materials and methods

### *2.1 Samples used (HFEs and radicals)*

1-fluoro-2-methoxypropane (HFE) and $BrO^{\bullet}$ radical were used for this computational investigation [2, 3, 13, 17, 25, 27]. The 3D structures of HFEs/radical were drawn using Spartan 14 v 114 suite licensed software [29].

### *2.2 Computational Procedures*

The Spartan 14 v 114 licensed software was used for all the electronic calculations. The geometry optimization of all chemical species involved in the reaction were carried out using density functional theory (DFT) based M06-2X method with the 6-311++G** basis set [27]. To improve the energy values, M06-2x/6-311++G(2df,2p) single-point calculations were immediately performed using same DFT method. Earlier related studies on computational kinetics showed that, theoretical thermochemistry and kinetics of reaction can be modeled accurately and provides reliable results when the DFT with M06-2X level of theory is employed [3, 5, 13, 17, 25, 32].

The minimum energy equilibrium structure obtained at each stationary point has all real frequencies meanwhile transition state possesses one imaginary frequency. The imaginary frequency in transition state corresponds to the coupling of stretching modes of the breaking C–H. Transformation from the reactant to product via the transition state (TS) along the minimum energy path was confirmed with the help of intrinsic reaction coordinate (IRC) calculations at the M06-2X level of DF theory [17]. IRC calculations confirmed the formation of pre and post-reaction complexes of the reactant/product molecule with the $BrO^{\bullet}$ radicals or HOBr in both the entry and exit of each reaction route.

The rate coefficients (k), change in enthalpy ($\Delta_r H^\circ_{rxn}$), change in free Gibb's energy ($\Delta_r G^\circ_{rxn}$) and change in energy ($\Delta_r E^\circ_{rxn}$) of each radical's reaction channels were computed according to the view of [28, 30] as in equation 10-14.

$$k = \sigma_r \Gamma \frac{k_B T}{h} \frac{Q_{TS}^{\dagger}}{Q_R} e^{-\frac{\Delta G^{\neq}}{RT}} \quad eq.10$$

The Arrhenius factor was computed using equation 11

$$A = \frac{k}{e^{-\frac{\Delta Ea^{\neq}}{RT}}} \quad eq.11$$

$$\Delta_r H^\circ_{rxn} = \sum_{prod.} \Delta_f H_{prod.} - \sum_{react.} \Delta_f H_{react.} \quad eq.12$$

$$\Delta_r G^\circ_{rxn} = \Delta_r H^\circ_{rxn} - T\Delta_r S^\circ_{rxn} \quad eq.13$$

$$\Delta_r E^\circ_{rxn} = \sum_{prod.} \Delta_f E_{prod.} - \sum_{react.} \Delta_f E_{react.} \quad eq.14$$

The change in enthalpy as well as Gibb's free energy of each transition states were estimated using expressions 15-16

$$\Delta H^{\#} = H^{\#} - \sum H_{reactants.} \quad eq.15$$

$$\Delta G^{\#} = G^{\#} - \sum G_{reactants.} \quad eq.16$$

The total rate coefficient was calculated using equation 17

$$k = k_{R_1} + k_{R_2} + k_{R_3} \quad eq.17$$

The branching ratios (BR) for the Hydrogen abstraction reaction channels of each radical, which is reported by [6] to have been represented the individual contribution of a reaction channel toward overall reaction rate were computed using an expression 18.

$$\text{Branching ratio} = \frac{k}{k_{Total}} * 100 \quad \text{eq.18}$$

The $E_a$ values of all reaction channels for each radical were determined using expression 19.

$$E_a = \Delta G^{\dagger} = \Delta H^{\#} - T\Delta S^{\#} \quad \text{eq.19}$$

The atmospheric lifetime of HFE + $^{\bullet}OH$ radical was computed using an expression 20

$$\tau_{eff} = \tau_{OH} \quad eq.20$$

The 100-time horizon Global warming potential (GWP) of HFE is estimated in accordance to the view of [3, 25] as expressed in equation 21.

$$GWP_i(H) = \frac{\int_0^H RF_i(t)dt}{\int_0^H RF_{CO_2}(t)dt} = \frac{AGWP_i(H)}{AGWP_{CO_2}(H)} \quad \text{eq. 21}$$

## 3. Results and Discussion

### *3.1 Sample conformers*

Fig. 1 shows the three possible conformers of 1-fluoro-2-methoxypropane molecule ranging from the lowest to highest energy conformers.

Monte Carlo's search was (conformational analysis) performed on $CFH_2CH(OCH_3)CH_3$ molecule by selecting Set up/Calculation/Conformational search under the application menu. MMFF force field was selected with maximum iteration number entered under the Mini tab. The default (1000) for maximum number was activated from the conformational search tab. The operation was then started with file name given. The result of this operational search showed nine conformers as illustrated in **Fig. 1.** From the analysis, the first conformer (88.90 kJ/mol) had the global minimum predicted. This search was aimed at identifying the possible conformers of $CFH_2CH(OCH_3)CH_3$ molecule with their respective global minima and to select the most stable conformer. Conformers with local minima were not considered since they are unstable [3, 17, 25]. The generated conformers were arranged in **Fig. 1** in order of increasing in their energy stabilities. So, with reference to **Fig. 1**, last conformer (107.67 kJ/mol) has the highest local minimum predicted and thus the most unstable.

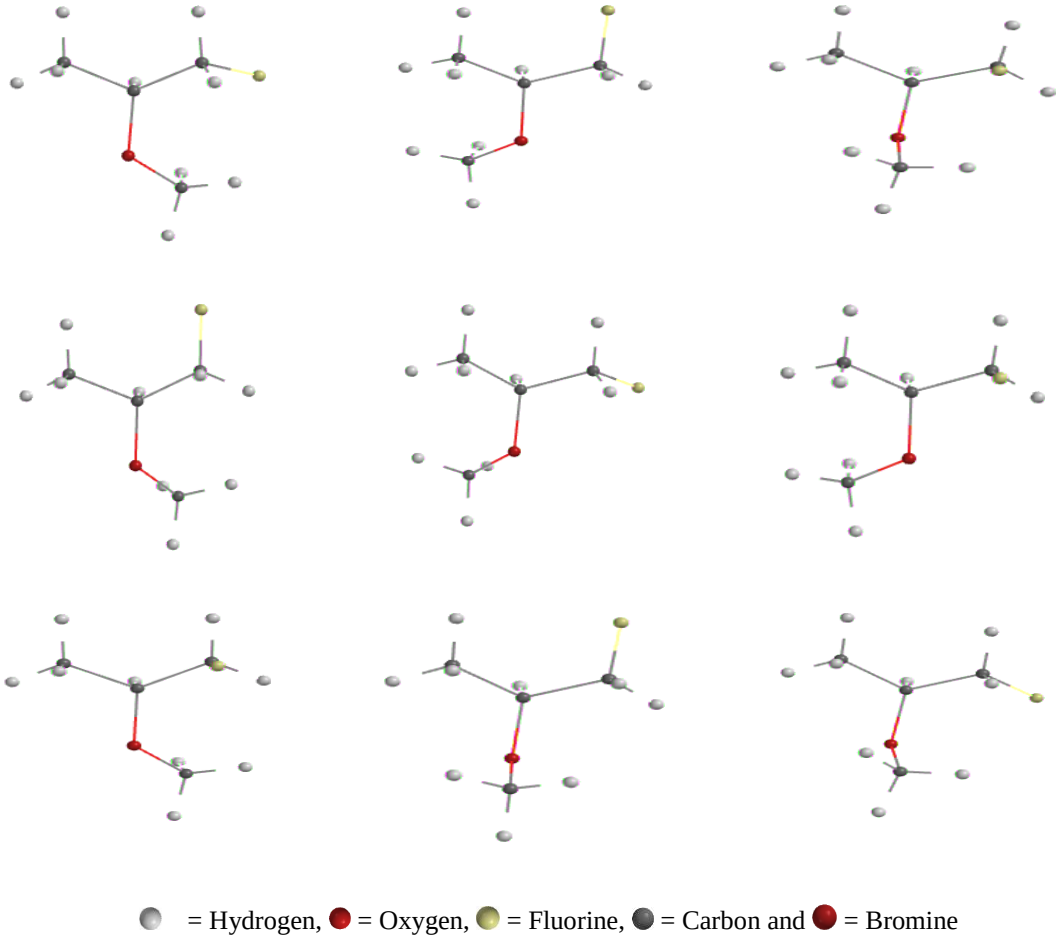


**Figure 1:** 3D structures of the possible conformers of 1-fluoro-2-methoxypropane molecule.

**Table 1:** DFT/M06-2X/6-311++G(2df,2p) calculated thermodynamic data on H-abstraction reaction channels (R1–R4) of 1-fluoro-2-methoxypropane with BrO•.

| **Reaction Routes** | $\Delta H^{\#}_{rxn}$ ($kJmol^{-1}$) | $\Delta S^{\#}_{rxn}$ ($J^{-1}molK$) | $\Delta G^{\#}_{rxn}$ ($kJmol^{-1}$) | $\Delta H^{o}_{rxn}$ ($kJmol^{-1}$) | $\Delta G^{o}_{rxn}$ ($kJmol^{-1}$) | $\Delta S^{o}_{rxn}$ ($J^{-1}molK$) |
|---|---|---|---|---|---|---|
| **R1** | -1.11 | -155.20 | 45.14 | -2.07 | -6.66 | 15.39 |
| **R2** | -2.86 | -157.69 | 44.13 | 1.19 | -4.89 | 20.40 |
| **R3** | -8.13 | -154.85 | 38.02 | -5.25 | -9.11 | 12.96 |
| **R4** | -3.80 | -157.62 | 43.17 | -1.56 | -3.99 | 8.17 |

The DFT/M06-2X/6-311++G(2df,2p) single-point calculation results presented in **Tables 1** (R1–R4) shows that, the reaction proceeded in four routes which can either be spontaneous or nonspontaneous in nature. The spontaneity and non-spontaneity of reaction via any route depends on the sign (i.e. + or -) of changes in enthalpy, entropy as well as Gibb's free energy of the reaction along the routes. The results also confirm the endothermic nature of reaction through R2 since $\Delta_r H°_{rxn} > 0$. Thus, Hydrogen abstraction along the R2 is thermodynamically unfavorable and reactions across R2 were nonspontaneous. While routes R1, R3 and R4 were exothermic in nature since $\Delta H_{rxn} < 0$ i.e. negative sign and thus, the reaction along the R1, R3 and R4 were thermodynamically favored, hence reaction across these routes were spontaneous. A spontaneous reaction is the one whose changes in enthalpy and Gibb's free energy are negatives and whose change in entropy is positive while non spontaneous is the whose changes in enthalpy and Gibb's free energy are positives and whose change in entropy is negative. In other hand, $\Delta_r G°_{rxn}$ and $\Delta_r S°_{rxn}$ across all reaction routes (R1-R4) proved the spontaneity of the reaction along the routes and justified all the final products through the routes to be thermodynamically feasible.

Also **Table 1** revealed that reaction of BrO• radical with the sample proceeded in two steps: (1) transition state formation and (2) product formation. On the basis of the Gibb's free energies of the two steps estimated in all routes, the rate determining step (RDS) of each reaction channel was identified on the basis of $\Delta G^{\#} > \Delta G_1$. Thus, first steps i.e. transition states formation across all reaction routes in Table 1 were the RDS.

The rate determining steps are the slowest steps in the reaction between the HFE and the BrO• radical investigated. $\Delta G^{\#}$ denotes change in Gibb's free energy of transition state formation while $\Delta G_1$ is the change Gibb's free energy of product formation.

**Table 2:** DFT/M06-2X/6-311++G(2df,2p) calculated kinetic data on H-abstraction reaction channels (R1–R4) of 1-fluoro-2-methoxypropane with BrO•

| **Reaction routes** | $k_{BrO}$ $(M^{-1}sec^{-1})$ | $Ea_{BrO}$ (kJ $mol^{-1}$) | $K * 10^{-1}$ | A $(M^{-1}sec^{-1})$ | $BR_{BrO}$ |
|---|---|---|---|---|---|
| **R1** | $2.24 * 10^{-11}$ | 2.48 | 9.82 | $2.24 * 10^{-11}$ | 28.18 |
| **R2** | $1.36 * 10^{-12}$ | 2.47 | 9.82 | $1.36 * 10^{-12}$ | 1.71 |
| **R3** | $3.42 * 10^{-11}$ | 2.47 | 9.85 | $3.42 * 10^{-11}$ | 43.02 |
| **R4** | $2.15 * 10^{-11}$ | 2.47 | 9.83 | $2.15 * 10^{-11}$ | 27.04 |

**Table 3:** DFT/M06-2X/6-311++G(2df,2p) calculated total rates ($k_T$), Atmospheric life time (ALT) and Global warming potentials (GWP) of 1-fluoro-2-methoxypropane system with BrO•

| **Radical** | $k_T$ $(M^{-1}sec^{-1})$ | **ALT (Day)** | **GWP** |
|---|---|---|---|
| **BrO** | $7.95*10^{-11}$ | $1.35*10^{-2}$ | 72.80 |

**Table 4:** DFT/M06-2X/6-311++G(2df,2p) calculated IRC on transition states of 1-fluoro-2-methoxypropane system reaction routes with BrO•

| **Reaction routes** | **Transition states ($TS_x$)** | **Intrinsic reaction coordinate ($cm^{-1}$)** |
|---|---|---|
| **R1** | TS1 | i575 |
| **R2** | TS2 | i480 |
| **R3** | TS3 | i343 |
| **R4** | TS4 | i525 |

Table 5: Variations in RC1-RC4 bond lengths during H-abstraction along the possible four reaction channels of 1-fluoro-2-methoxypropane with BrO•

| RC1 | Bond length (Å) | RC2 | Bond length (Å) | RC3 | Bond length (Å) | RC4 | Bond length (Å) |
|---|---|---|---|---|---|---|---|
| **C1,F1** | 1.364 | C1,F1 | 1.366 | C1,F1 | 1.394 | C1,F1 | 1.370 |
| **C2,O1** | 1.431 | C2,O1 | 1.503 | C2,O1 | 1.450 | C2,O1 | 1.449 |
| **Br1,O2** | 1.878 | Br1,O2 | 1.862 | Br1,O2 | 1.868 | Br1,O2 | 1.886 |
| **C4,O1** | 1.481 | C4,O1 | 1.427 | C4,O1 | 1.420 | C4,O1 | 1.419 |
| **C2,C3** | 1.526 | C2,C3 | 1.625 | C2,C3 | 1.529 | C2,C3 | 1.605 |
| **C1,C2** | 1.530 | C1,C2 | 1.663 | C1,C2 | 1.606 | C1,C2 | 1.534 |

**Table 6:** Variations in TS1-TS4 bond lengths during H-abstraction along the possible four reaction channels of 1-fluoro-2-methoxypropane with BrO•

| TS1 | Bond length (Å) | TS2 | Bond length (Å) | TS3 | Bond length (Å) | TS4 | Bond length (Å) |
|---|---|---|---|---|---|---|---|
| **C1,F1** | 1.363 | C1,F1 | 1.365 | C1,F1 | 1.388 | C1,F1 | 1.372 |
| **C2,O1** | 1.433 | C2,O1 | 1.468 | C2,O1 | 1.440 | C2,O1 | 1.435 |
| **Br1,O2** | 1.877 | Br1,O2 | 1.864 | Br1,O2 | 1.862 | Br1,O2 | 1.879 |
| **C4,O1** | 1.485 | C4,O1 | 1.430 | C4,O1 | 1.423 | C4,O1 | 1.420 |
| **C2,C3** | 1.530 | C2,C3 | 1.615 | C2,C3 | 1.528 | C2,C3 | 1.545 |
| **C1,C2** | 1.533 | C1,C2 | 1.587 | C1,C2 | 1.608 | C1,C2 | 1.536 |

**Table 7:** Variations in PC1-PC4 bond lengths during H-abstraction along the possible four reaction channels of 1-fluoro-2-methoxypropane with BrO•

| PC1 | Bond length (Å) | PC2 | Bond length (Å) | PC3 | Bond length (Å) | PC4 | Bond length (Å) |
|---|---|---|---|---|---|---|---|
| **C1,F1** | 1.377 | C1,F1 | 1.372 | C1,F1 | 1.368 | C1,F1 | 1.373 |
| **C2,O1** | 1.435 | C2,O1 | 1.417 | C2,O1 | 1.423 | C2,O1 | 1.428 |
| **Br1,O2** | 1.874 | Br1,O2 | 1.860 | Br1,O2 | 1.856 | Br1,O2 | 1.875 |
| **C4,O1** | 1.380 | C4,O1 | 1.430 | C4,O1 | 1.415 | C4,O1 | 1.418 |
| **C2,C3** | 1.528 | C2,C3 | 1.589 | C2,C3 | 1.525 | C2,C3 | 1.567 |
| **C1,C2** | 1.525 | C1,C2 | 1.589 | C1,C2 | 1.573 | C1,C2 | 1.542 |
| **H11O2** | 1.064 | H11O2 | 1.065 | H11O2 | 1.064 | H11O2 | 1.065 |

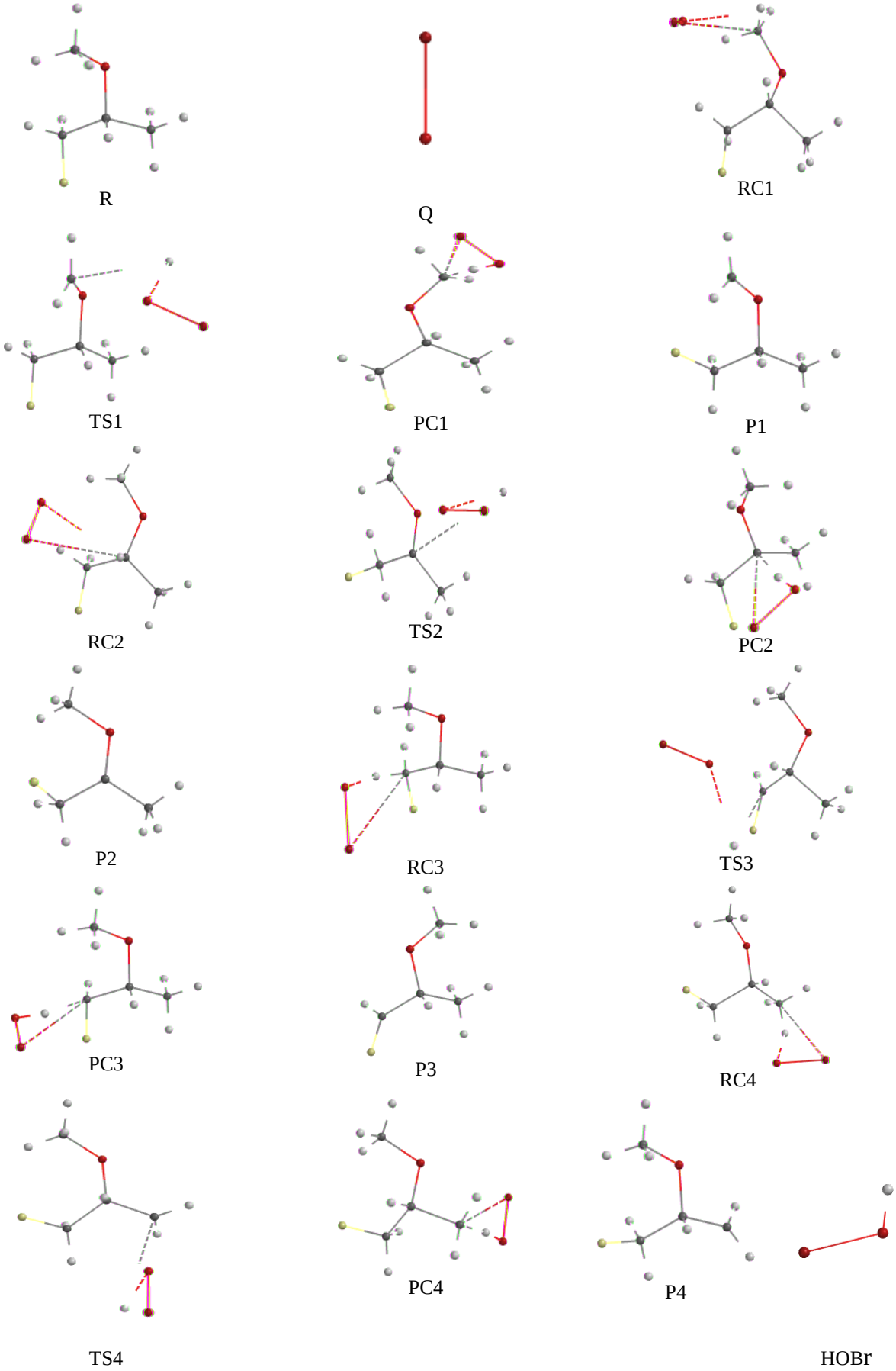


**Figure 2:** Optimized geometries for 1-fluoro-2-methoxypropane system with Bromine monoxide radical (BrO•)

**Table 8:** Variations in RC1-RC4 bond angles during H-abstraction along the possible four reaction channels of 1-fluoro-2-methoxypropane system with BrO•

| RC1 | Bond angle (°) | RC2 | Bond angle (°) | RC3 | Bond angle (°) | RC4 | Bond angle (°) |
|---|---|---|---|---|---|---|---|
| **<C1F1H2** | 31.72 | <C1F1H2 | 32.10 | <C1F1H2 | 37.94 | <C1F1H2 | 31.80 |
| **<C1H1H2** | 35.81 | <C1H1H2 | 36.62 | <C1H1H2 | 20.25 | <C1H1H2 | 35.31 |
| **<C1F1H1** | 31.45 | <C1F1H1 | 31.91 | <C1F1H1 | 39.22 | <C1F1H1 | 31.86 |
| **<C1C2C3** | 110.19 | <C1C2C3 | 110.31 | <C1C2C3 | 115.92 | <C1C2C3 | 109.85 |
| **<C1C2O1** | 112.80 | <C1C2O1 | 91.07 | <C1C2O1 | 112.39 | <C1C2O1 | 112.24 |
| **<C2O1C4** | 112.08 | <C2O1C4 | 110.24 | <C2O1C4 | 112.73 | <C2O1C4 | 113.00 |
| **<Br1O2H9** | 85.45 | <Br1O2H5 | 84.01 | <Br1O2H1 | 84.79 | <Br1O2H7 | 83.51 |
| **<O1C4O2** | 123.50 | <O1C4O2 | 76.28 | <O1C4O2 | 53.83 | <O1C4O2 | 34.20 |
| **<C4O2Br1** | 58.84 | <C2O2Br1 | 58.89 | <C1O2Br1 | 59.30 | <C3O2Br1 | 58.43 |

**Table 9:** Variations in TS1-TS4 bond angles during H-abstraction along the possible four reaction channels of 1-fluoro-2-methoxypropane system with BrO•

| TS1 | Bond angle (°) | TS2 | Bond angle (°) | TS3 | Bond angle (°) | TS4 | Bond angle (°) |
|---|---|---|---|---|---|---|---|
| **<C1F1H2** | 32.14 | <C1F1H2 | 31.67 | <C1F1H2 | 26.53 | <C1F1H2 | 31.77 |
| **<C1H1H2** | 35.30 | <C1H1H2 | 35.45 | <C1H1H2 | 35.12 | <C1H1H2 | 35.29 |
| **<C1F1H1** | 32.14 | <C1F1H1 | 31.76 | <C1F1H1 | 41.26 | <C1F1H1 | 31.80 |
| **<C1C2C3** | 111.97 | <C1C2C3 | 122.67 | <C1C2C3 | 112.36 | <C1C2C3 | 113.17 |
| **<C1C2O1** | 109.77 | <C1C2O1 | 115.96 | <C1C2O1 | 112.50 | <C1C2O1 | 112.50 |
| **<C2O1C4** | 112.66 | <C2O1C4 | 118.87 | <C2O1C4 | 112.58 | <C2O1C4 | 112.58 |
| **<C11O2H9** | 170.81 | <C11O2H4 | 166.08 | <C11O2H7 | 169.07 | <Cl1O2H7 | 169.07 |
| **<O1C4O2** | 107.01 | <O1C4O2 | 87.04 | <O1C4O2 | 37.67 | <O1C4O2 | 37.67 |
| **<C4O2C11** | 163.40 | <C2O2C11 | 167.99 | <C1O2C11 | 160.49 | <C3O2Cl1 | 163.44 |

**Table 10:** Variations in PC1-PC4 bond angles during H-abstraction along the possible four reaction channels of 1-fluoro-2-methoxypropane system with BrO•

| PC1 | Bond angle (°) | PC2 | Bond angle (°) | PC3 | Bond angle (°) | PC4 | Bond angle (°) |
|---|---|---|---|---|---|---|---|
| **<C1F1H2** | 31.58 | <C1F1H2 | 31.74 | <C1F1H2 | 36.77 | <C1F1H2 | 31.65 |
| **<C1H1H2** | 35.72 | <C1H1H2 | 35.88 | <C1H1H2 | 35.28 | <C1H1H2 | 35.14 |
| **<C1F1H1** | 31.53 | <C1F1H1 | 31.67 | <C1F1H1 | 47.92 | <C1F1H1 | 31.79 |
| **<C1C2C3** | 112.02 | <C1C2C3 | 99.15 | <C1C2C3 | 112.18 | <C1C2C3 | 112.36 |
| **<C1C2O1** | 113.19 | <C1C2O1 | 101.64 | <C1C2O1 | 110.83 | <C1C2O1 | 112.80 |
| **<C2O1C4** | 117.70 | <C2O1C4 | 116.40 | <C2O1C4 | 113.13 | <C2O1C4 | 113.11 |
| **<Br1O2H11** | 79.69 | <Br1O2H11 | 78.61 | <Br1O2H11 | 80.55 | <Br1O2H11 | 79.04 |
| **<O1C4O2** | 97.34 | <O1C4O2 | 53.12 | <O1C4O2 | 62.96 | <O1C4O2 | 34.73 |
| **<C4O2Br1** | 59.97 | <C2O2Br1 | 59.89 | <C1O2Br1 | 60.27 | <C3O2Br1 | 60.13 |

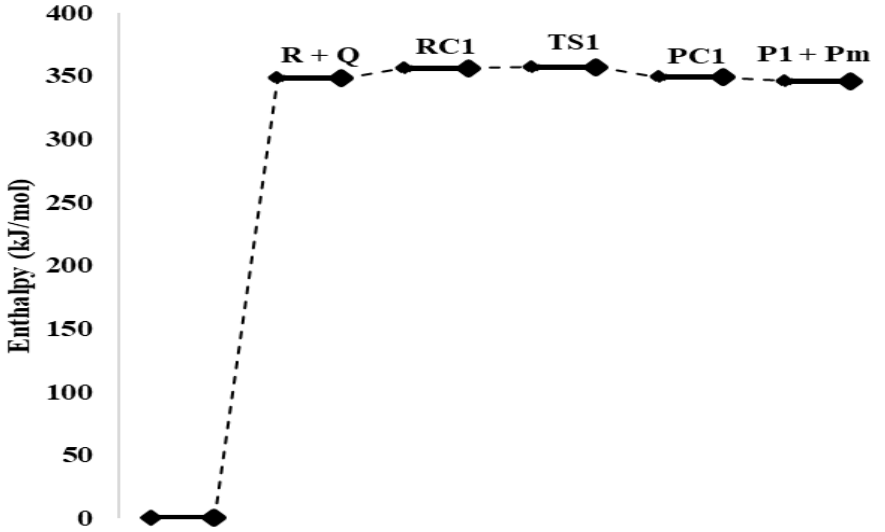


**Fig. 3**: Energy profile diagram of 1-fuoro-2-methoxypropane with BrO˙ through $R_1$

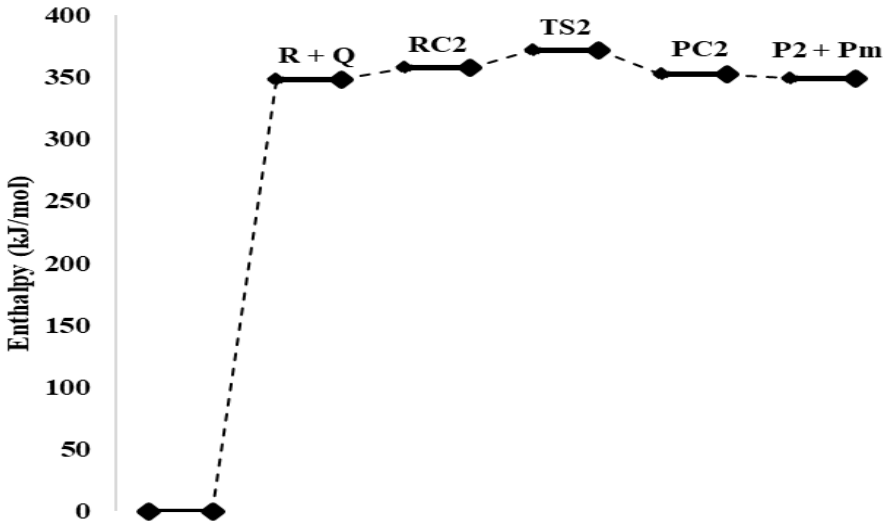


**Fig. 4:** Energy profile diagram of 1-fuoro-2-methoxypropane with BrO˙ through $R_2$

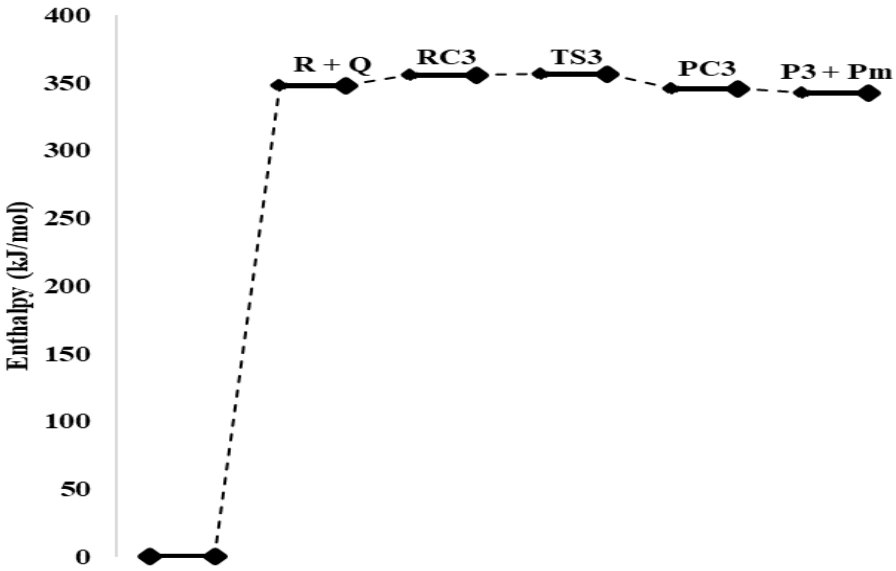


**Fig. 5:** Energy profile diagram of 1-fuoro-2-methoxypropane with BrO˙ through $R_3$

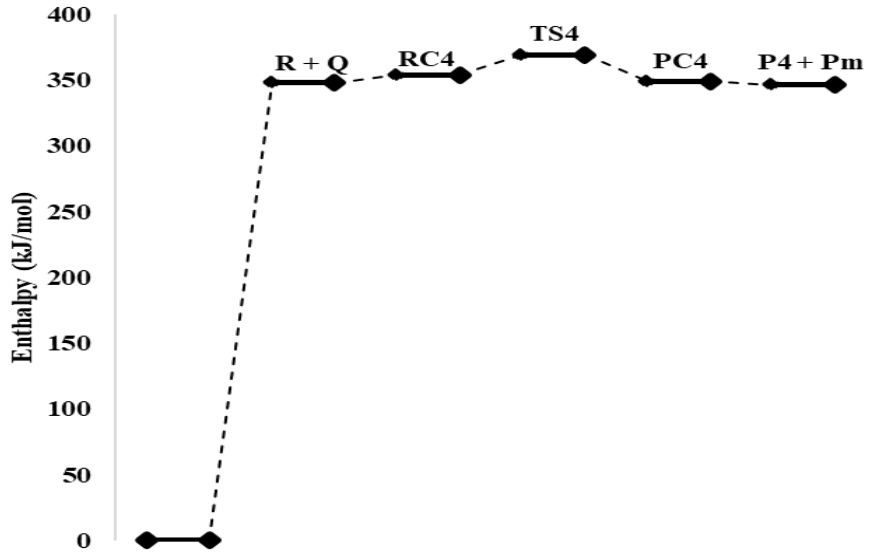


**Fig. 6:** Energy profile diagram of 1-fuoro-2-methoxypropane with BrO˙ through $R_4$

As presented in Table 2, the rate constant (k), activation energy ($E_a$), equilibrium constant (K), Arrhenius factor (A) and Branching ratio (BR) of the reaction between 1-fluoro-2-methoxypropane with BrO˙ radical. The computed rates of reaction along the four routes increase in order $k_3 > k_1 > k_4 > k_2$. The route R3 possessed higher rate which implies that, the reaction along R3 was faster owing to the fact that, the higher the rate constant of a reaction the faster the reaction as reported by [28]. The total rate of $7.95*10^{-11}$ $M^{-1}sec^{-1}$ was recorded.

Furthermore, the equilibrium constants (K) and activation energy ($E_a$) across all the reaction routes decreased and increased alternately while the branching ratio which entails the individual chemical contribution of each radical reaction routes toward overall theoretical rates computed also decreased and increased alternately across reaction routes. Similarly, it was discovered that, the alternate change in branching ratios followed the higher the rate, the higher the branching ratios and vice versa.

As presented in the Table 3, the computed ALT of 1-fluoro-2-methoxypropane with atmospheric radical BrO˙. Assuming the atmospheric BrO˙ concentration as $1.08*10^7$ M [1, 3], the 1-fluoro-2-methoxypropane GWPs was computed relative to the $CO_2$ reference information using an eq. 21.

The computed GWP as well as ALT obtained for 1-fluoro-2-methoxypropane vs BrO˙ radical reaction in 100-year time horizon were $1.35*10^{-2}$ day/72.80 while the GWP for CFC-11, the most vital CFC with numerous applications (100-year time horizon) was reported as 4600 [3]. By chemical comparison and implication, an investigated system with shorter estimated atmospheric lifetime and GWP is of lesser atmospheric and environmental effects than CFCs, thus 1-fluoro-2-methoxypropane can serve as good substantial substitute for CFCs.

The presented results in Table 4 show the careful examination of vibrational motion and an intrinsic reaction coordinates (IRC) calculation performed on all transition states at the same level. This was done in order to prove the chemical connection between the transition states, reactants as well as products of reaction for each route. The minimum energy equilibrium structure obtained at each stationary point has all real frequencies meanwhile transition state possesses one imaginary frequency. These imaginary frequencies in the transition states correspond to the coupling of stretching modes cleavage of C–H. The IRC calculation performed also confirmed the chemical transformation of reactant to product via the transition state (TS) along the minimum energy path. IRC calculations also served as chemical evidence for the formation of pre and post-reaction complexes of the reactant/product molecule with the radicals or minor products of the reaction in both the entry and exit of each route.

The optimized structures of the sample with selected atmospheric radical is shown in the Figures **2.**

Tables 5-10 show the variations in bond lengths and angles of the reactant complexes, transition states and product complexes as reaction progressed to products.

The energy profile diagram of each reaction route of 1-fluoro-2-methoxypropane with the Bromine monoxide radical are presented in Figures 3-6.

## 4. Conclusions

In this computational kinetic investigation, it was observed that the reaction of 1-fluoro-2-methoxypropane with BrO˙ followed many routes and depend on number of Hydrogen environments in the investigated system. The reaction proceeded by oxidation and led to Hydrogen abstraction. The oxidation of this sample with the investigated radical was spontaneous along all the possible routes on the

basis of changes in Gibb's free energy as well as the entropy of the reaction. On the basis of change in enthalpy of reaction, R1, R3 and R4 were more favored while R2 was less favored.

The reaction rate along all the identified routes decreased in the order of $k_3 > k_1 > k_4 > k_2$. This implies that oxidation through R3 was the fastest while R2 was the least. This also account for less favorability nature of oxidation through R2. The total theoretical rate of $7.95*10^{-11}$ $M^{-1}$ $sec^{-1}$ was recorded while the ALT and GWP estimated were reasonably very low which justified 1-fluoro-2-methoxypropane as a substantial substitute for CFCs.

**Acknowledgement**

Mohammed Rufai Abubakar acknowledges the financial support of Petroleum Technology Development Fund (PTDF), Abuja, Nigeria, for providing a PTDF M.Sc. award (Award Letter No:PTDF/ED/LSS/MSc/MRA/

244/17

**References**

[1] J. G. Anderson, W. H. Brune, S. A. Lloyd, D. W. Toohey, S. P. Sander, W. L. Starr, M. Loewenstein, J. R. Podolske, Kinetics of $O_3$ Destruction by ClO and BrO within the Antarctic Vortex: An Analysis Based on in Situ ER-2 Data, *J. of Geophysical Research*, 94 (1989) 11,480-11,520.

[2] J.G. Anderson, FREE RADICALS IN THE EARTH'S ATMOSPHERE: Their Measurement and Interpretation, *Ann. Rev. Phys. Chem.*, 38 (1987) 489-520.

[3] B. Baidya, M. Lily, A. K. Chandra, Theoretical study on atmospheric chemistry of $CHF_2CF_2CH_2OH$: Reaction with OH radicals, lifetime and global warming potentials, *Computational and Theoretical Chem.*, 1119 (2017) 1 – 9.

[4] L. K. Christensen, J. Sehested, O. J. Nielsen, M. Bilde, T. J. Wallington, A. Guschin, L. T. Molina, M. J. Molina, Atmospheric Chemistry of HFE-7200 ($C_4F_9OC_2H_5$): Reaction with OH Radicals and Fate of $C_4F_9OCH_2CH_2O(•)$ and $C_4F_9OCHO(•)CH_3$ Radicals, *J. Phys. Chem. A.*, 102 (1998) 4839-4845.

[5] E. F. V. De Carvalho, O. Roberto-Neto, Effects of Multidimensional Tunneling in the Kinetics of Hydrogen Abstraction Reactions of O ($^3$P) with $CH_3OCHO$, *Journal of Computational Chem.*, (2018) 1-9.

[6] R. C. Deka, B. K. Mishra, Theoretical studies on kinetics, mechanism and thermochemistry of gas – phase reactions of HFE – 449mec-f with OH radicals and Cl atom, *J Mol Graph and Model.*, 53 (2014) 23-30.

[7] J. Espinosa-Garcia, Ab Initio and Variational Transition – State Theory of the $CF_3CF_2OCH_3$ + OH Reaction Using Integrated Methods: Mechanism and Kinetics, *J. Phys. Chem. A.*, 107 (2003) 1618- 1626.

[8] A. Galano, J. R. Alvarez-Idaboy, M. Francisco-Marquez, Mechanism and Branching Ratio of Hydroxyl Ethers + OH Gas Phase Reactions: Relevance of H Bond Interactions, *J. Phys. Chem. A.*, 144 (2003) 7525-7536.

[9] E. Garfield, Ozone-Layer Depletion: Its Consequences, the Causal Debate, and International Cooperation, *Essays of an Information Scientist: Science Literacy, Policy, Evaluation and other Essays*, 11 (1988) 39-49.

[10] D. A. Good, J. S. Francisco, A. K. Jain, D. J. Wuebbles, Lifetime and global warming potentials for Dimethyl ether and for fluorinated ethers: $CH_3OCH_3$ (E143a), $CHF_2OCHF_2$ (E134), $CHF_2OCF_3$ (E125), *Journal of Geophysical Research*, 103 (1998) 28,186-28,186.

[11] N. K. Gour, B. K. Mishra, I. Hussaini, R. C. Deka, Theoretical Investigation on the kinetics and Thermochemistry of H-atom abstraction reactions of 2-chloroethyl methyl ether ($CH_3OCH_2CH_2Cl$) with OH radical at 298 K, *Struct. Chem.*, (2016) 1 – 9.

[12] Q. Guo, N. Zhang, T. Uchimaru, L. Chen, H. Quan, J. Mizukado, Atmospheric chemistry of cyc-$CF_2CF_2CF_2CH=CH–$: Kinetics, products, and mechanism of gas-phase reaction with OH radicals, and atmospheric implications, *Atmospheric Environment*, 179 (2018) 69-76.

[13] S. R. Hashemi, V. Saheb, Theoretical Studies on the Mechanism and Kinetics of the Hydrogen Abstraction Reactions of threo- $CF_3CHFCHFC_2F_5$ and erthro-$CF_3CHFCHFC_2F_5$ (HFC-43-10mee) by OH radicals, *Computational & Theoretical Chemistry*, (2017) 1-28.

[14] M. D. Hurley, T. J. Wallington, M. P. S. Andersen, D. A. Ellis, J. W. Martin, S. A. Mabury, Atmospheric Chemistry of Fluorinated Alcohols: Reaction with Cl Atoms and OH Radicals and Atmospheric, *J. Phys. Chem. A.*, 108 (2004) 1973-1979.

[15] B. Laszlo, E. H. Robert, J. K. Michael, W. M. Andrzej, Kinetic studies of the reactions of BrO and IO radicals, *Journal of Geophysical Research*, 102 (1997) 1523-1532.

[16] S. A. M a b u r y, C. J. Young, M. D. Hurley, T. J. Wallington, Atmospheric Lifetime and Global Warming Potential of a Perfluoropolyether, *Environ. Sci. Technol*., 40 (2006) 2242-2246.

[17] R. A. Mohammed, U. Adamu, S. G. Gideon, S. Uba, Computational kinetic study on atmospheric oxidation reaction mechanism of 1-fluoro-2-methoxypropane with OH and ClO radicals, *Journal of King Saud University–Science*, (2018) xxx-xxx. DOI: doi.org/10.1016/j.jksus.2018.08.011.

[18] J. M. Molina, F. S. Rowland, Stratospheric sink for chlorofluoromethanes: chlorine atom-catalyzed destruction of ozone, *Nature*, 249 (1974) 810-812.

[19] V. L. Orkin, E. Villenave, R. E. Huie, M. J. Kurylo, Atmospheric Lifetimes and Global Warming Potentials of Hydrofluoroethers: Reactivity toward OH, UV Spectra, and IR Absorption Cross Sections, *J. Phys. Chem. A.*, 103 (1999) 9770-9779.

[20] F. F. Østerstrøm, T. J. Wallington, O. J. Nielsen, M. P. S. Andersen, Atmospheric Chemistry of $(CF_3)_2CHOCH_3$, $(CF_3)_2CHOCHO$, and $CF_3C(O)OCH_3$, *J. Phys. Chem. A.*, 119 (2015) 1256-1666.

[21] V. C. Papadimitriou, D. K. Papanastasiou, V. G. Stefanopoulos, A. M. Zaras, Y. G. Lazarou, P. Papagiannakopoulos, Kinetics study of the Reactions of Cl Atoms with $CF_3CH_2CH_2OH$, $CF_3CF_2CH_2OH$, $CHF_2CF_2CH_2OH$ and $CF_3CHFCF_2CH_2OH$, *J. Phys. Chem. A.*, 111 (2007) 11608 – 11617.

[22] M. Prather, C. M. Spivakovsky, Tropospheric OH and the Lifetimes of Hydrochlorofluorocarbons, *Journal of Geophysical Research*, 95 (1990) 18,723-18,729.

[23] F. Rohrer, H. Berresheim, Strong correlation between levels of Tropospheric hydroxyl radical and solar ultraviolet radiation, *Nature*, 442 (2006) 184-187.

[24] F. S. Rowland, Stratospheric Ozone depletion, *Phil. Trans. R. Soc. B*., 361 (1996) 769-790.

[25] M. A. Rufai, U. Adamu, A. G. Shallangwa, S. Uba, An Insilco study of 1,1-difluoro-2-methoxypropane reaction mechanism with the Bromine monoxide (BrO) radical, *Journal of Engineering and Exalt Sciences*, 04 (2018) 0404-0413.

[26] T. Sako, M. Sato, N. Nakazawa, M. Oowa, M. Yasumoto, H. Ito, S. Yamashita, Critical Properties of Fluorinated Ethers, *J. Chem. Eng. Data*, 41 (1996) 802-805.

[27] H. Schlager, V. Grewe, A. Roiger, Chemical composition of the atmosphere, *Springer*, (2012) 17-35

[28] A. A. Siaka, A. Uzairu, A. Idris, H. Abba, Thermodynamics and Kinetics of Spiro – Heterocycle Formation Mechanism: Computational Study, *Phys. Chem. Res.*, 5(3) (2017) 439-446.

[29] Spartan '14 v 114, (2013) Wave function, Inc., Irvine.

[30] D. G. Truhlar, B. C. Garrett, S. J. Klippenstein, Current Status of Transition-State Theory, *J. Phys. Chem.*, 100 (1996) 12771-12800.

[31] Y-N. Wang, J. Chen, X. Li, B. Wang, X. Cai, L. Huang, Predicting rate constants of hydroxyl radical reactions with organic pollutants: Algorithm, Validation, applicability domain and mechanistic interpretation, *Atmospheric Environment*, 43 (2009) 1131-1135.

[32] C. W. White, J. M. Martell, Hydrogen Abstraction from Fluorinated Ethyl Methyl Ether System by OH Radicals, *Advances in Physical Chemistry*, (2015) 1-10.

[33] L. Yang, J-Y. Liu, L. Wang, H-Q. He, Y. Wang, Z-S. Li, Theoretical Study of the Reactions $CF_3CH_2OCHF_2$ + OH/Cl and its Product Radicals and Parent Ether ($CH_3CH_2OCH_3$) with OH, *J Comput Chem.* 29 (2007) 550–561.

[34] J-T. Ye, F-Y. Bai, X-M. Pan, Computational Study of H-abstraction reactions from $CH_3OCH_2CH_2Cl$/$CH_3CH_2OCH_2CH_2Cl$ by Cl atom and OH radical and fate of alkoxy radicals, *Environ. Sci. Pollut. Res.*, 23 (2016) 23467–23484.

## How to Cite This Article

Rufai Abubakar Mohammed; Uzairu Adamu; Uba Sani; Shallangwa Adamu Gideon; Azeh Yakub. "Thermodynamics and kinetics of 1-fluoro-2-methoxypropane vs Bromine monoxide radical (BrO): A computational view". Chemical Review and Letters, 2, 3, 2019, 107-117. doi: 10.22034/crl.2019.185789.1013